This article has been accepted for publication in a future issue of this journal, but has not been fully edited. Content may change prior to final publication. Citation information: DOI 10.1109/LAWP.2021.3068393, IEEE Antennas and Wireless Propagation Letters

Probabilistic attenuation nowcasting for the 5G telecommunication networks

Jayaram Pudashine, Carlos Velasco-Forero, Mark Curtis, Adrien Guyot, Valentijn R.N. Pauwels, Jeffrey P. Walker, and Alan Seed

***Abstract*—In this paper, we propose a novel approach to produce attenuation forecasts for microwave links using a probabilistic approach. It uses ensembles of forecast rainfall fields to easily derive attenuation forecasts for specific frequencies. The proposed approach uses the Short Term Ensemble Prediction System (STEPS) to generate ensembles of high, spatial and temporal, resolution forecast rainfall fields based on observed weather radar fields with lead times of 15 to 90 minutes. Attenuation forecasts could eventually be used by telecommunication operators to drive the operation of wireless networks and ensure their maintenance during severe and extreme rainfall events. This study used 109 microwave links ranging from 15 to 40 GHz to verify the results of this probabilistic attenuation forecast. Results suggest that the STEPS-based attenuation forecasts were within the narrow span of the 90 percent confidence region for all microwave links tested up to 30-minute lead time, decreasing for longer lead times. Examples of how the proposed approach can be used to derive detailed probabilistic attenuation forecast for multiple lead times within a domain of few kilometers, as well as probability of attenuation maps for large areas are shown.**

***Index Terms*— attenuation, 5G mobile communication, wireless communication.**

I. INTRODUCTION

WIRELESS communication providers are currently facing an unprecedented challenge to meet the user demand for high-speed data transfer [1]. This is putting significant pressure on the available spectrum allocations of telecommunication operators and to its existing backhaul networks. Currently, mobile carriers are relying on frequencies from 700 MHz to 8 GHz which are almost at saturation level [2]; thus the wireless providers have been rolling out the fifth-generation (5G) wireless communication in recent years. Studies have showed that millimetre wave (1 mm to 10 mm) frequencies ranging from 30 to 300 GHz could be used to supplement the saturated spectrum bands for wireless communication [1]. However, these millimetre wave frequencies suffer more signal attenuation when the electromagnetic wave propagates through the air than at the longer wavelengths, mostly due to oxygen absorption and liquid precipitation. Precipitation or rainfall is a flux of water measured in kilogram per square meter which is derived based on the drop size distribution and the fall velocity of the rain drops. Also, the attenuation due to this flux is a function of the size and distribution of rain droplets [3]. This poses additional challenges to the telecommunication engineers who must design efficient and reliable networks to meet user demands. Moreover, the existing backhaul networks need to be upgraded to higher frequencies to handle the greater data volumes, whereby rainfall will again have a significant impact on signal attenuation, particularly during heavy rainfall events.

To overcome the impact of rainfall, 5G networks are likely to be deployed in a dense cell with a radius of few hundreds of meters. The International Telecommunication Union (ITU) developed a model to compute the probability of rain rates at various geographical locations using historical data [3]. However, extreme rainfall is inevitable and predicted to be more frequent in a changing climate [4], so the ITU model may not represent future or current conditions. Accordingly, innovative ideas have been proposed to address these issues so as to ensure the resiliency of an operational network during extreme weather conditions [5, 6]. One of the propositions is to periodically update the network topology [7–9] and other is to use rain-related link states to improve the routing mechanism [10, 11]. Both of these ideas used *a priori* information on the attenuation of the future conditions of the links which were based on the radar echoes of rainfall. Thus, having a reliable and timely short-term rainfall prediction (also known as *nowcast*) could be helpful for designing a more resilient wireless network during extreme weather conditions. Thanks to the well-described and robust power relationship between rainfall and attenuation [3, 12, 13], predicted rainfall can easily be converted to attenuation for a given frequency.

The term *nowcast* is commonly used for providing early warnings of extreme events like floods and landslides [14]. Usually, this term refers to the forecast of precipitation or other weather variables like wind or temperature, at high spatial and temporal resolutions (1-10 min and 100-1000 m) with short lead times (minutes to a few hours) which can provide sufficient time and information for rapid response during hazardous weather events. Examples of operational rainfall nowcasting systems are the Short-Term Ensemble Prediction System (STEPS) [15], RADVOR [16], and SWIRLS [17]. A python-based open-source probabilistic nowcasting tool called pySTEPS is also available and used essentially in research setups [18]. These probabilistic nowcast rainfall products have mainly been used for hydrological forecasting [19–21] to predict and warn about flash and riverine flooding, and there has been some topical usage in the aviation industry [22, 23]. However, rainfall nowcast data has never been used or tested

J. Pudashine, C. Velasco-Forero and M. Curtis are with the Bureau of Meteorology, Radar Science and Nowcasting team, Melbourne, Australia, email : jayaram.pudashine@bom.gov.au; carlos.velasco@bom.gov.au; mark.curtis@bom.gov.au

A. Guyot, J.P. Walker and V.R.N, Pauwels are with the Department of Civil Engineering, Monash University, Clayton, Australia, email: adrien.guyot@monash.edu; jeff.walker@monash.edu; valentijn.pauwels@monash.edu

A. Seed is with Griffith University, School of Engineering and Built Environment, Brisbane, Australia, email: a.seed@griffith.edu.au

This article has been accepted for publication in a future issue of this journal, but has not been fully edited. Content may change prior to final publication. Citation information: DOI 10.1109/LAWP.2021.3068393, IEEE Antennas and Wireless Propagation Letters

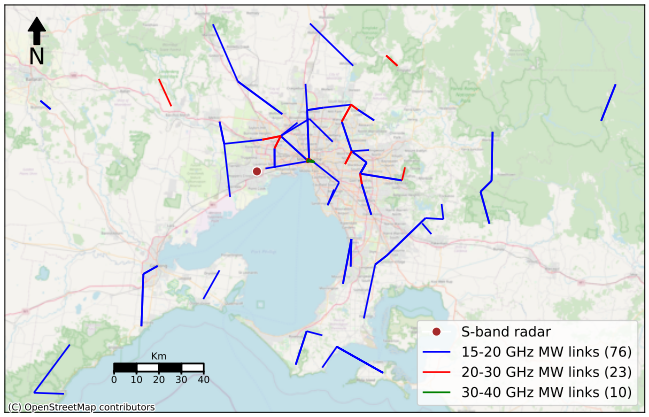

Fig. 1. Microwave links from one operator for Greater Melbourne. The sub-panel on the top-right shows microwave links above 30 GHz which are located mainly around the Melbourne CBD. The Melbourne operational (S-band) radar is located at Laverton (-37.852°, 144.752°) *(Source of the background map: OpenStreetMap).*

for designing the topology of microwave links or their real-time operation as a wireless communication network. This paper provides for the very first time a spatial probabilistic attenuation forecast, which could be used by telecommunication operators for designing and real-time decision making of their networks. Consequently, the primary objective is to demonstrate the potential of using short-term attenuation forecast data by mobile network operators in operating and maintaining wireless networks.

II. STUDY AREA AND DATASETS

The study site covered the Greater Melbourne area in the Australian state of Victoria. The dataset used here contains minimum, maximum and average Received signal level (RSL) data over 15-minute intervals, from one of the cellular communication operators within a radius of 200 km around the City of Melbourne. A total of 109 microwave links (including duplex links, lengths from 0.2 to 22 km) with a frequency > 15 GHz were selected for this study, as shown in Fig. 1. Among the 109 links, 98 links were duplex, and 11 links were single-channel links with a total of 60 unique links. These links were grouped into three distinct frequency ranges, 15-20 GHz (76 links), 20-30 GHz (23 links), and $>$ 30 GHz (10 links). The rainfall dataset used here contains 10 rainfall events (including both convective and stratiform rainfall) between October 2019 and April 2020. The detail of these events and selection criteria are described in [24]. The 5-minute, 500-meter, rainfall fields named *Rainfields* [25] were produced using weather radar data from the Australian Bureau of Meteorology S-Band operational weather radar located at Laverton (-37.852°, 144.752°) as shown in Fig. 1; refer to [25] for the detail quality control of these products. For this study, the reference path averaged rainfall was obtained by taking the average of the overlaying cells of the rain field data along the path segment.

III. METHODS

A. Rainfall Nowcasting: Short Term Ensemble Prediction System (STEPS)

STEPS uses a multiplicative cascade scale decomposition approach to generate high-resolution ensembles of rainfall forecasts from weather radar rainfall observations for a short period (usually up to 60 to 90 minutes ahead) [15, 26]. The main goal of STEPS is that any predicted rainfall field exhibits similar space-time structures to those of observed rainfall fields over a range of space and time scales. STEPS was formulated to blend an advection forecast from radar observations with a noise model possessing the space-time properties of observed rain fields [15, 27, 28]. In this study, the STEPS method was used to predict ensembles of rainfall fields up to 90 minutes ahead. For a deeper review of the history of rainfall nowcasting and its evolution to the probabilistic framework used in this study, please refer to [28].

B. Estimating attenuation from rainfall

Fundamental studies of rain-induced attenuation on microwave signals have shown that at any given microwave frequency, the rainfall-attenuation relationship [3, 12, 13] can be accurately approximated as a power law following $k = \alpha \mathrm{R}^{\beta}$, where, α and β are the coefficients dependent on the frequency and polarisation of the microwave signal. Here, rain-induced attenuation, also known as specific attenuation, is denoted by k and typically expressed in logarithmic units of decibels per kilometre (dB km^{-1}) with rainfall rate R expressed in millimeters per hour (mm h^{-1}). Default values of the two parameters are provided by the ITU-Radiocommunication [3]. However, for this study local parameters were obtained based on three years of continuous drop size distribution data, as collected by disdrometers located within Greater Melbourne [29]. Also, to note, that the impact of temperature on the signal attenuation is very minimal compared with the attenuation due to rain [9, 30], thus this has not been considered separately in this analysis.

C. Estimating probabilistic forecast attenuation

The proposed approach in this paper is to use the Short Term Ensemble Prediction System (STEPS) to generate ensembles of high, spatial and temporal, resolution forecast rainfall fields from the latest observed radar rainfall fields for lead times of 15 to 90 minutes. Then, forecast attenuation for the frequency of interest can be derived from these predicted rainfall rates simply by using the rainfall-attenuation relationship (III-B). As each location has already multiple possible predicted values of rainfall for each lead time, multiple possible attenuation values can be derived at each location. As it is shown in the results section, these ensembles of forecast attenuation values can be processed to derive probabilistic products such as expected forecast attenuation along microwave links, chance of exceedance of a given attenuation threshold in a small area and for each location across large regions, among others.

D. Attenuation retrieval from CML data

In order to verify the quality of the here-proposed forecast attenuation technique, the algorithm proposed by [31] was used to derive attenuation from observed 15-minute RSL dataset from Commercial Microwave Links (CML). This algorithm was developed for rainfall retrieval from commercial microwave links. A brief description is given below:

This article has been accepted for publication in a future issue of this journal, but has not been fully edited. Content may change prior to final publication. Citation information: DOI 10.1109/LAWP.2021.3068393, IEEE Antennas and Wireless Propagation Letters

a) Wet/Dry classification was based on the gauge-adjusted radar data. Time steps for which the rainfall rate from radar was greater than or equal to 0.1 mm h^{-1} were considered as wet, and the remaining time steps were considered as dry.

b) Baseline signal was obtained based on the moving median of the received signal level for the previous 24-hour dry period.

c) Attenuation was obtained by deducting the baseline signal from the received signal level. The result obtained was the specific attenuation which was then multiplied with the total path length to obtain the total link attenuation.

E. Evaluation Metrics

i) Root Mean Square Error: The root mean square error (RMSE) was calculated per lead-time as $\sqrt{\sum_{i=1}^{N}(F_i - O_i)^2/N}$, where are forecast and observed attenuation at a given grid cell, and N corresponds to the number of forecasts with the lead time t. RMSE has the same unit as the observation and forecast, with lower values indicating better performance.

ii) Receiver Operating Characteristics : The receiver operating characteristics (ROC) curve provides a measure of the predictive ability of a certain attenuation threshold with the probabilistic forecast. For any event, the ROC curve can be plotted with the probability of detection vs false alarm rate for a predefined probability. For a skillful forecast, the curve passes above the 1:1 line. Also the area under the ROC curve is used to determine the skill of the forecast; when the area is above 0.8 is considered excellent and above 0.9 outstanding [32].

IV. RESULTS

To show the feasibility of using high spatial and temporal resolution rainfall nowcast data (STEPS) for forecasting attenuation at the individual link level, Fig. 2 illustrates one typical example of probabilistic attenuation predictions with 90% confidence interval for a 37.61 GHz link (length of 1.38 km) during one of the rainfall events. For lead times of 30-minutes, the confidence regions covered most of the observed attenuation data well with a narrow span, indicating that the forecast attenuation was both correct and useful. As expected, as lead time increases to 60 and 90 minutes the confidence interval (CI) range widened indicating less confidence in the attenuation prediction.

Fig. 3 and 4 illustrate how an ensemble rainfall forecast obtained from STEPS can be converted to probabilistic attenuation forecast that could be further utilised to derive the exceedance probability of attenuation within a cell size of a few kilometres. Fig. 3a shows the forecast rainfall field from 2020-01-15 06:15 with a lead time of 15 minutes with a fast-moving convective system passing across the Melbourne central business district during this time. A single member taken randomly from the 96-member rainfall ensemble is shown. Fig. 3b shows a zoomed-in area within which a strong spatial contrast in the rainfall intensity within 50 km radius was observed. Here, one section of 2 km x 2 km was selected for this analysis, labeled as 'cell A'. Although, a similar approach can be

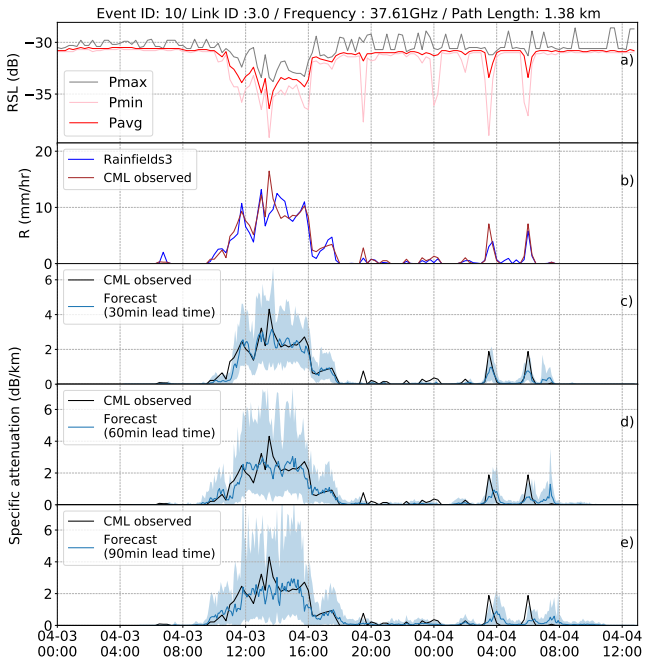

Fig. 2. Example of a time series plot for a CML above 30 GHz (37.61 GHz with link length of 1.38 km) showing (a) minimum (Pmin), maximum (Pmax) and average (Pavg) observed RSL data (b) comparison of rainfall estimates based on radar and CML attenuation. Observed vs forecast (mean) attenuation for (c) 30 min lead time (d) 60 min lead time; and (e) 90 min lead time with 90 % confidence interval shaded in blue for event 10 (2020-04-03 00:00 to 14:00 UTC).

applied for regions of any sizes and shapes. Rainfall intensities obtained within cell A were converted to specific attenuation for 65 GHz. Since STEPS produced 96 ensemble members, a probabilistic representation of attenuation could be represented by an attenuation exceedance probability function. Figure 4a shows the complementary cumulative distribution function for the attenuation of all the grid points within the 2 km cell for four different lead times, 15, 30, 45 and 60 minutes. Results shown that for cell A there is a 30% chance of exceeding 20 dB of attenuation for 15-minute lead time that grew up to a 40% chance for a 30-minute lead time and then reduced back to 20% chance for 60-minute lead time. As this was a fast-moving convective system, these distributions in the expected attenuation for different lead times are likely associated to the uncertainty in the expected arrival time and the intensity of heavy precipitation into the cell. This analysis for a single cell can be extended to all locations in the area of study to construct a map, with probability of attenuation exceeding a given threshold between points which are for example 500 m apart. Fig. 4b shows the probability of exceedance of an attenuation of 2 dB km^{-1} at 65 GHz for a lead time of 30 minutes at a spatial resolution of 500 meters. From the Fig. 4b, areas with a higher probability of occurrence of attenuation can be easily distinguished for this lead time. This information can be used to estimate the total expected attenuation of a link connecting any two locations within the study area, with those links using the highest frequency likely to be more attenuated.

To further understand the performance of the attenuation forecast for all links and rainfall events in the dataset, root mean square error (RMSE) for three frequency groups of the microwave links are presented in Fig. 5 for lead times from

This article has been accepted for publication in a future issue of this journal, but has not been fully edited. Content may change prior to final publication. Citation information: DOI 10.1109/LAWP.2021.3068393, IEEE Antennas and Wireless Propagation Letters

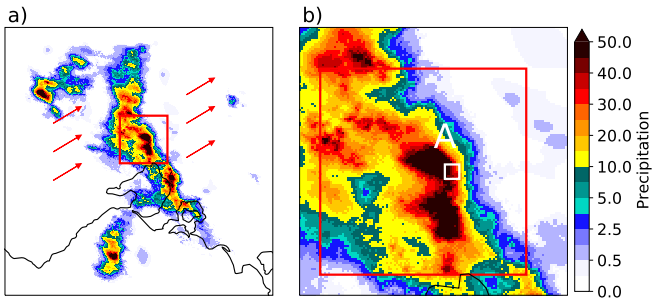

Fig. 3. (a) Forecast rainfall field obtained from one of the ensemble members at 2020-01-15 06:30 UTC (15-min lead time forecast from 2020-01-15 06:15). Red arrow indicates the direction of rainfall field. (b) Zoomed section showing the high variability of the rainfall field.

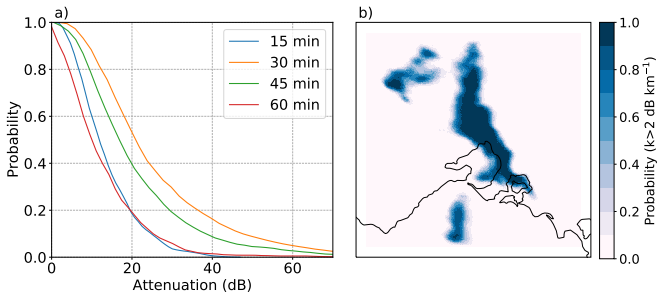

Fig. 4. (a) Cumulative distribution function of attenuation for different lead times for 65 GHz within a radius of 2km from the center of a cell. (b) Probability of attenuation between points 500 m apart for a threshold of 2 dB km-1 and lead time of 30 minutes for 65 GHz.

15 to 90 minutes. As expected, RMSE for all three groups increased with the lead time, however the extent of the spread of the 90 % confidence interval for frequency groups above 30 GHz was higher than for the two other groups. Indeed, higher frequency links suffered more from attenuation and presented more noise in the RSL data as compared to the lower frequency microwave links. In addition, the magnitude of the average RMSE was also higher for the higher frequency groups.

As an example for all three frequency groups of microwave links, Fig. 6 shows the ROC curve for a 2 dB km^{-1} attenuation threshold for different lead times. For all frequency groups, the ROC curves were closer to the top left corner of the diagram showing the ability to detect the probability of occurrence of an attenuation above 2 dB km^{-1}. This can also be explained by the fact that the area under the ROC curve for all groups and all lead times were higher than 0.79 (in the range of excellent skill). Moreover, microwave links with a frequency above 30 GHz showed better performance with higher ROC area compared to the two other groups (for lead times up to 60 minutes; areas under the curve are higher than 0.9 which is an outstanding skill of forecast). This is because higher frequency microwave links are subjected to higher attenuation from rainfall and higher noise to signal ratio than lower frequency links. Also based on [33], there are other factors such as elevation of Fresnel zone above the ground, nature of ground surface, atmospheric propagation conditions, antenna heights can also have some impact on signal attenuation. However, many of these factors are difficult to dissociate and

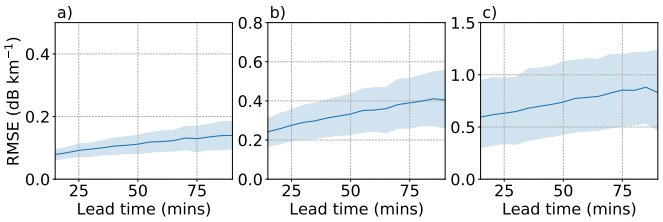

Fig. 5. RMSE based on 10 rainfall events as a function of lead time for: (a) links between 15 to 20 GHz; (b) links between 20 to 30 GHz; and (c) links above 30 GHz.

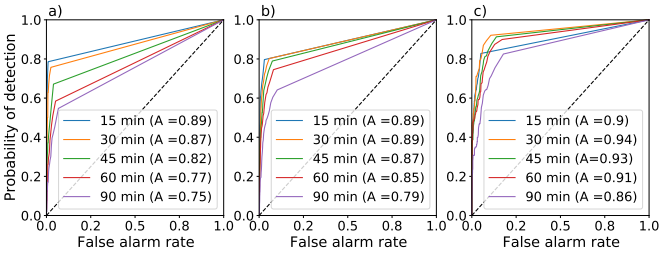

Fig. 6. ROC curves for different lead times with a threshold of 2 dB km^{-1} for link frequency groups: (a) 15 to 20 GHz; (b) 20 to 30 GHz; and (c) above 30 GHz.

the main contributing factor is mainly due to precipitation and atmospheric propagation conditions.

V. CONCLUSIONS

The main aim of this study was to investigate the feasibility of using high spatial and temporal resolution rainfall nowcast data for forecasting attenuation at the individual link level. This was achieved by verifying the forecast against the observed attenuation obtained from 109 links based on 10 rainfall events. Results showed that proposed rainfall-based attenuation nowcast was able to predict observed attenuation within the narrow 90 percent confidence interval for all of the microwave links for up to 30-minute lead time. Confidence in attenuation forecast decreased for longer lead times, with some variability across individual events and microwave links. This study also provided an example of probabilistic attenuation map within a domain of few kilometers (likely resolution of interest for the 5G network) and for the entire radar coverage. This analysis was based on 10 rainfall events with most of the events occurring during the summer season, and so it does not cover the seasonal variation. Shorter and high-frequency links are likely to be more affected by high intensity fast-moving convective cells than widespread low-intensity rainfall, thus future research should focus on performing verification of such probabilistic forecast on tropical areas. Although, the primary use of the nowcast rainfall data is to provide a reliable and timely prediction of extreme weather rainfall, this study has shown that attenuation forecasts can be derived as a by-product of that weather prediction with minimal additional effort. As this methodology is solely based on radar observation, this may not be feasible in the area where there is no radar coverage and there are uncertainties in the radar observation itself due to the ground clutter, anomalous propagation and beam spreading [34] which will impact the attenuation forecast.

REFERENCES

[1] T. S. Rappaport, S. Sun, R. Mayzus, H. Zhao, Y. Azar, K. Wang, G. N. Wong, J. K. Schulz, M. Samimi, and F. Gutierrez, "Millimeter wave mobile communications for 5g cellular: It will work!" *IEEE Access*, vol. 1, pp. 335–349, 2013.

[2] H. B. Hamid Dutty and M. M. Mowla, "Weather impact analysis of mmwave channel modeling for aviation backhaul networks in 5g communications," in *2019 22nd International Conference on Computer and Information Technology (ICCIT)*, 2019, pp. 1–6.

[3] ITU-R, *Recommendation ITU-R P.838-3*, 2005.

[4] M. Tippett, "Extreme weather and climate," *npj Climate and Atmospheric Science*, vol. 1, no. 1, p. 45, 2018.

[5] J. Rak, P. E. Heegaard, and B. E. Helvik, "Resilience of communication networks to random failures and disasters: An optimization perspective," *Networks*, vol. 75, no. 4, pp. 337–339, June 2020. [Online]. Available: https://doi.org/10.1002/net.21940

[6] M. Pióro, E. Fitzgerald, I. Kalesnikau, D. Nace, and J. Rak, "Optimization of wireless networks for resilience to adverse weather conditions," in *Computer Communications and Networks*. Springer International Publishing, 2020, pp. 523–556. [Online]. Available: https://doi.org/10.1007/978-3-030-44685-7_21

[7] J. Rak, "A new approach to design of weather disruption-tolerant wireless mesh networks," *Telecommunication Systems*, vol. 61, no. 2, pp. 311–323, Apr. 2015. [Online]. Available: https://doi.org/10.1007/s11235-015-0003-z

[8] J. Rak, M. Pickavet, K. S. Trivedi, J. A. Lopez, A. M. C. A. Koster, J. P. G. Sterbenz, E. K. Çetinkaya, T. Gomes, M. Gunkel, K. Walkowiak, and D. Staessens, "Future research directions in design of reliable communication systems," *Telecommunication Systems*, vol. 60, no. 4, pp. 423–450, Mar. 2015. [Online]. Available: https://doi.org/10.1007/s11235-015-9987-7

[9] M. Tornatore, J. Andre, P. Babarczi, T. Braun, E. Folstad, P. Heegaard, A. Hmaity, M. Furdek, L. Jorge, W. Kmiecik, C. M. Machuca, L. Martins, C. Medeiros, F. Musumeci, A. Pasic, J. Rak, S. Simpson, R. Travanca, and A. Voyiatzis, "A survey on network resiliency methodologies against weather-based disruptions," in *2016 8th International Workshop on Resilient Networks Design and Modeling (RNDM)*. IEEE, Sept. 2016. [Online]. Available: https://doi.org/10.1109/rndm.2016.7608264

[10] A. Jabbar, J. P. Rohrer, V. S. Frost, and J. P. Sterbenz, "Survivable millimeter-wave mesh networks," *Computer Communications*, May 2011. [Online]. Available: https://doi.org/10.1016/j.comcom.2011.05.011

[11] F. Yaghoubi, M. Furdek, A. Rostami, P. Oehlen, and L. Wosinska, "Reliable topology design of wireless networks under correlated failures," in *2018 IEEE International Conference on Communications (ICC)*, 2018, pp. 1–6.

[12] D. Atlas, R. C. Srivastava, and R. S. Sekhon, "Doppler radar characteristics of precipitation at vertical incidence," *Reviews of Geophysics*, vol. 11, no. 1, p. 1, 1973. [Online]. Available: https://doi.org/10.1029/rg011i001p00001

[13] R. Olsen, D. Rogers, and D. Hodge, "The arb correlation in the calculation of rain attenuation," *IEEE Transactions on Antennas and Propagation*, vol. 26, no. 2, pp. 318–329, Mar. 1978. [Online]. Available: https://doi.org/10.1109/tap.1978.1141845

[14] G. Ayzel, T. Scheffer, and M. Heistermann, "RainNet v1.0: a convolutional neural network for radar-based precipitation nowcasting," *Geoscientific Model Development*, vol. 13, no. 6, pp. 2631–2644, June 2020. [Online]. Available: https://doi.org/10.5194/gmd-13-2631-2020

[15] N. E. Bowler, C. E. Pierce, and A. W. Seed, "STEPS: A probabilistic precipitation forecasting scheme which merges an extrapolation nowcast with downscaled NWP," *Quarterly Journal of the Royal Meteorological Society*, vol. 132, no. 620, pp. 2127–2155, Oct. 2006. [Online]. Available: https://doi.org/10.1256/qj.04.100

[16] T. Winterrath, W. Rosenow, and E. Weigl, "On the dwd quantitative precipitation analysis and nowcasting system for real-time application in german flood risk management," in *Weather and Radar Hydrology*, vol. 351. Exeter, UK: IAHS Publ, 2011.

[17] P. Cheung and H. Yeung, "Application of optical-flow technique to significant convection nowcast for terminal areas in hong kong," in *The 3rd WMO International Symposium on Nowcasting and very short range forecasting (WSN12)*, Rio de Janeiro, Brazil, 2012.

[18] S. Pulkkinen, D. Nerini, A. A. P. Hortal, C. Velasco-Forero, A. Seed, U. Germann, and L. Foresti, "Pysteps: an open-source python library for probabilistic precipitation nowcasting (v1.0)," *Geoscientific Model Development*, vol. 12, no. 10, pp. 4185–4219, Oct. 2019. [Online]. Available: https://doi.org/10.5194/gmd-12-4185-2019

[19] M. L. Poletti, F. Silvestro, S. Davolio, F. Pignone, and N. Rebora, "Using nowcasting technique and data assimilation in a meteorological model to improve very short range hydrological forecasts," *Hydrology and Earth System Sciences*, vol. 23, no. 9, pp. 3823–3841, Sept. 2019. [Online]. Available: https://doi.org/10.5194/hess-23-3823-2019

[20] R. Ferretti, A. Lombardi, B. Tomassetti, L. Sangelantoni, V. Colaiuda, V. Mazzarella, I. Maiello, M. Verdecchia, and G. Redaelli, "A meteorological–hydrological regional ensemble forecast for an early-warning system over small apennine catchments in central italy," *Hydrology and Earth System Sciences*, vol. 24, no. 6, pp. 3135–3156, June 2020. [Online]. Available: https://doi.org/10.5194/hess-24-3135-2020

[21] D. Heuvelink, M. Berenguer, C. C. Brauer, and R. Uijlenhoet, "Hydrological application of radar rainfall nowcasting in the netherlands," *Environment International*, vol. 136, p. 105431, Mar. 2020. [Online]. Available: https://doi.org/10.1016/j.envint.2019.105431

[22] K. Sheth, T. Amis, S. Gutierrez-Nolasco, B. Sridhar, and D. Mulfinger, "Development of probabilistic convective weather forecast threshold parameter for flight routing decisions," NASA Ames Research Center, Tech. Rep., 2013.

[23] R. Osinski and F. Bouttier, "Short-range probabilistic forecasting of convective risks for aviation based on a lagged-average-forecast ensemble approach," *Meteorological Applications*, vol. 25, no. 1, pp. 105–118, Nov. 2017. [Online]. Available: https://doi.org/10.1002/met.1674

[24] C. Velasco-Forero, J. Pudashine, M. Curtis, and A. Seed, "Steps3-adv verification report," Bureau of Meteorology, Tech. Rep. 978-1-925738-20-9, September 2020 2020.

[25] A. Seed, C. Leahy, E. Duthie, and S. Chumchean, "Rainfields : The australian bureau of meteorology system for quantitative precipitation estimation, and it's use in hydrological modelling," in *Proceedings of Water Down Under 2008*, M. Lambert, T. Daniell, and M. Leonard, Eds. Modbury, SA: Engineers Australia, 2008, pp. 661–670.

[26] A. W. Seed, "A dynamic and spatial scaling approach to advection forecasting," *Journal of Applied Meteorology*, vol. 42, no. 3, pp. 381–388, Mar. 2003. [Online]. Available: https://doi.org/10.1175/1520-0450(2003)042⟨0381:adassa⟩2.0.co;2

[27] N. E. Bowler, C. E. Pierce, and A. Seed, "Development of a precipitation nowcasting algorithm based upon optical flow techniques," *Journal of Hydrology*, vol. 288, no. 1-2, pp. 74–91, Mar. 2004. [Online]. Available: https://doi.org/10.1016/j.jhydrol.2003.11.011

[28] A. W. Seed, C. E. Pierce, and K. Norman, "Formulation and evaluation of a scale decomposition-based stochastic precipitation nowcast scheme," *Water Resources Research*, vol. 49, no. 10, pp. 6624–6641, Oct. 2013. [Online]. Available: https://doi.org/10.1002/wrcr.20536

[29] A. Guyot, J. Pudashine, A. Protat, R. Uijlenhoet, V. R. N. Pauwels, A. Seed, and J. P. Walker, "Effect of disdrometer type on rain drop size distribution characterisation: a new dataset for south-eastern australia," *Hydrology and Earth System Sciences*, vol. 23, no. 11, pp. 4737–4761, Nov. 2019. [Online]. Available: https://doi.org/10.5194/hess-23-4737-2019

[30] J. Luomala and I. Hakala, "Effects of temperature and humidity on radio signal strength in outdoor wireless sensor networks," in *Proceedings of the 2015 Federated Conference on Computer Science and Information Systems*. IEEE, Oct. 2015. [Online]. Available: https://doi.org/10.15439/2015f241

[31] A. Overeem, H. Leijnse, and R. Uijlenhoet, "Retrieval algorithm for rainfall mapping from microwave links in a cellular communication network," *Atmospheric Measurement Techniques*, vol. 9, no. 5, pp. 2425–2444, June 2016. [Online]. Available: https://doi.org/10.5194/amt-9-2425-2016

[32] D. W. Hosmer and S. Lemeshow, *Applied Logistic Regression*. John Wiley & Sons, Inc., Sept. 2000. [Online]. Available: https://doi.org/10.1002/0471722146

[33] A. Guyot, J. Pudashine, A. Protat, R. Uijlenhoet, V. R. N. Pauwels, V. Louf, and J. P. Walker, "Wildfire smoke particulate matter concentration measurements using radio links from cellular communication networks," *AGU Advances*, 2021. [Online]. Available: https://doi.org/10.1029/2020AV000258

[34] A. Berne and W. Krajewski, "Radar for hydrology: Unfulfilled promise or unrecognized potential?" *Advances in Water Resources*, vol. 51, pp. 357–366, Jan. 2013. [Online]. Available: https://doi.org/10.1016/j.advwatres.2012.05.005